Original Article

Trans-portal hepatic infusion of cultured bone marrow-derived mesenchymal stem cells in a steatohepatitis murine model

Ryo Sasaki,[1] Taro Takami,[1,2,*] Koichi Fujisawa,[3] Toshihiko Matsumoto,[4] Tsuyoshi Ishikawa,[1] Naoki Yamamoto,[5] and Isao Sakaida[1,2,3]

[1]Department of Gastroenterology and Hepatology, [2]Center for Regenerative and Cell Therapy, [3]Department of Liver Regenerative Medicine and [4]Department of Oncology and Laboratory Medicine, Yamaguchi University Graduate School of Medicine, Ube, Yamaguchi, 1-1-1 Minami Kogushi, Ube, Yamaguchi 755-8505, Japan
[5]Yamaguchi University Health Administration Center, 1-1-1 Minamikogushi, Ube, Yamaguchi 755-0046, Japan

(Received 27 May, 2020; Accepted 13 June, 2020; Published online 30 September, 2020)

The incidence of nonalcoholic steatohepatitis-related liver cirrhosis is increasing. We used a steatohepatitis murine model fed a choline-deficient, L-amino acid-defined (CDAA) diet with a single injection of carbon tetrachloride (CCl_4) to evaluate the efficacy of trans-portal hepatic infusion of bone marrow-derived mesenchymal stem cells (BMSCs) for liver fibrosis, liver steatosis, and oxidative stress. Mice were fed a CDAA diet and injected with a single intraperitoneal dose of CCl_4 (0.5 ml/kg) after 4 weeks of CDAA diet. After 12 weeks of CDAA diet, 1×10^6 luciferase-positive syngeneic BMSCs (Luc-BMSCs) were infused into the animal spleen. An *in vivo* imaging system was used to confirm Luc-BMSC accumulation in the liver via the portal vein, and at 4 weeks after infusion, we compared liver fibrosis, liver steatosis, and oxidative stress. After the BMSC-infusion, serum albumin and serum total bilirubin were significantly improved. Liver fibrosis assessed by Sirius red staining, α-smooth muscle actin protein, and collagen 1A1 mRNA expression was significantly suppressed. Furthermore, liver steatosis area was significantly lower, the 8-hydroxy-2'-deoxyguanosine-positive cells were significantly fewer, and superoxide dismutase 2 protein expression of the liver was significantly increased. In conclusion, our data confirmed the efficacy of trans-portal hepatic infusion of BMSCs in a steatohepatitis murine model.

***Key Words*: mesenchymal stem cell, nonalcoholic steatohepatitis, liver fibrosis, oxidative stress, macrophage polarization**

Chronic liver injury caused by the hepatitis B virus (HBV), hepatitis C virus (HCV), nonalcoholic steatohepatitis (NASH), and alcohol leads to the progression of hepatic fibrosis and eventually liver cirrhosis. Currently, liver transplantation remains the radical treatment for decompensated liver cirrhosis. We previously reported that the infusion of whole bone-marrow cells to a murine model of carbon tetrachloride (CCl_4)-induced liver fibrosis caused lysis of the existing liver fibrosis, consistent with improved liver functions and better survival rate. Since then, we have conducted clinical research on autologous bone marrow cell infusion therapy for the treatment of decompensated liver cirrhosis.[1–3] We have also used murine and canine models of liver fibrosis to evaluate the efficacy of cultured bone marrow-derived mesenchymal stem cells (BMSCs) in the treatment of decompensated liver cirrhosis and have developed a cultured BMSC hepatic artery infusion therapy that is less invasive and gives more sustained therapeutic effects.[4–6]

Given that the recent establishment of nucleoside/nucleotide analogs (NAs) and direct-acting antiviral (DAA) therapies has allowed us to control HBV and elucidate HCV, we anticipate an increasing number of liver cirrhosis cases caused by NASH. NASH-related liver cirrhosis and NASH-related hepatocellular carcinoma are already the second most common indications for liver transplantation in the United States;[7,8] thus, preventing NASH is an important topic. Many reports cite liver fibrosis as the most important factor for liver disease-related death in non-alcoholic fatty liver disease (NAFLD) and NASH,[9–11] although despite the existence of therapeutic drugs such as peroxisome proliferator-activator receptor (PPAR) agonists, statins, and vitamin E that target liver steatosis, inflammation, and oxidative stress, there remains no approved effective therapy against liver fibrosis. Here, we used a steatohepatitis murine model fed a choline-deficient, L-amino acid-defined (CDAA) diet with a single injection of CCl_4 to evaluate the efficacy of trans-portal hepatic infusion of syngeneic cultured BMSCs in treating liver fibrosis and liver steatosis.

Material and Methods

Modified steatohepatitis murine model. B6N-Tyr$^{c\text{-}Brd}$/BrdCrCrl mice (B6 albino) were purchased from Charles River Laboratories Japan, Inc. (Kanagawa, Japan). The mice were maintained in specific pathogen-free housing at the Animal Experiment Facility of the Yamaguchi University School of Medicine. All experiments were conducted in accordance with the Guidelines for Animal Experiments of Yamaguchi University School of Medicine after obtaining approval for the experimental protocol (Approval number: 21-S13). Our protocol for the modified steatohepatitis murine model fed a CDAA diet with a single injection of CCl_4 is shown in Fig. 1A. Ten-week-old male B6 albino mice were fed a CDAA diet (#518753; Dyets Inc., Bethlehem, PA) for 4 weeks, then injected a single intraperitoneal dose of CCl_4 (Wako, Osaka, Japan) at 0.5 ml/kg to induce lobular inflammation and fibrosis in the liver based on the model of Komiya *et al.*[12] The CDAA diet was continued after CCl_4 injection, and 12 weeks later, the mice were sacrificed, and their livers were harvested to compare intra-hepatic inflammation and steatosis with mice not injected with CCl_4.

Luciferase-positive (Luc-BMSC) preparation. B6 mouse-derived BMSCs (passage 6) purchased from Cyagen Biosciences Inc. (Tokyo, Japan) were transduced with lentiviral vectors (#79692-G; BPS Bioscience, San Diego, CA) expressing luciferase, and passage 8 BMSCs (Luc-BMSCs) were used in the experi-

*To whom correspondence should be addressed.
E-mail: t-takami@yamaguchi-u.ac.jp

doi: 10.3164/jcbn.20-88

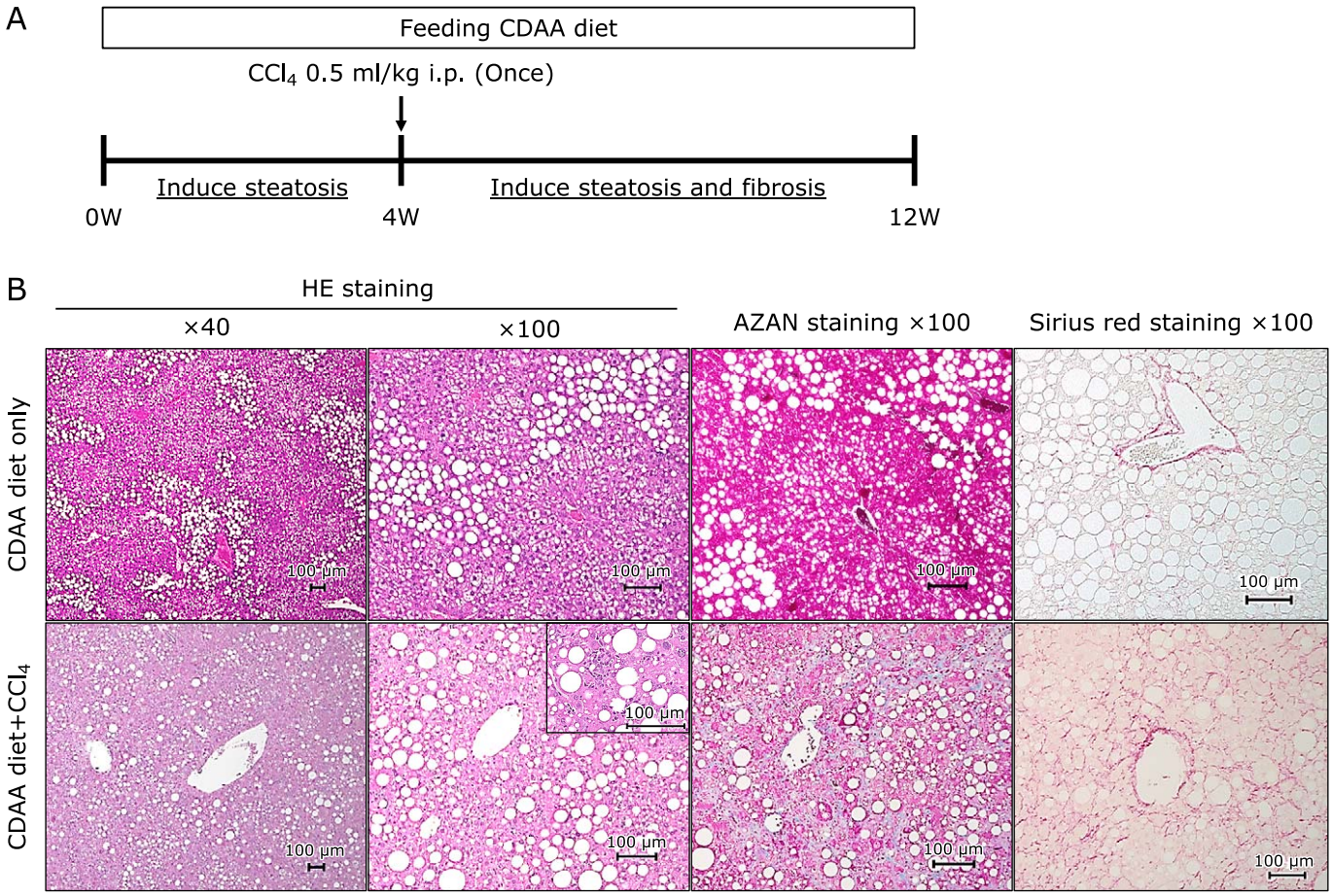

Fig. 1. Modified steatohepatitis murine model protocol. (A) Model protocol. Mice are fed a choline-deficient L-amino acid-defined (CDAA) diet for 4 weeks and then injected a single intraperitoneal dose of carbon tetrachloride (CCl_4) at 0.5 ml/kg. The CDAA diet is continued thereafter, and the mice are sacrificed after 12 weeks of the CDAA diet (12W). (B) Hematoxylin and eosin (HE) staining (magnification ×40, ×100, ×200), AZAN staining (magnification ×100), and Sirius red staining (magnification ×100) of the liver. Scale bars = 100 μm.

mentation. The culture medium used was Dulbecco's Modified Eagle Medium (DMEM) (Thermo Fisher Scientific, Waltham, MA) with 10% fetal bovine serum (FBS) (Thermo Fisher Scientific), and 100 μg/ml of gentamicin (Thermo Fisher Scientific) added. BMSCs were cultured at 37°C under 5% CO_2. Before infusion, BMSCs were reacted with 0.25% trypsin-EDTA (# 25200-072; Thermo Fisher Scientific) at 37°C for 5 min, dissociated from the culture dish, and then adjusted to 1.0×10^6 cells/100 μl with phosphate-buffered saline (PBS) (Thermo Fisher Scientific).

Experimental protocol. After 12 weeks of CDAA diet (or 8 weeks after CCl_4 injection), the modified steatohepatitis model mice were anesthetized with ISOFLURANE Inhalation Solution (Pfizer, Tokyo, Japan), and Luc-BMSCs (1.0×10^6 cells/body) were infused into the spleen. Mice were then injected with 150 μg/body of luciferin (E160A; Promega Corporation, Madison, WI) into the caudal vein, and an *in vivo* imaging system (IVIS Spectrum BL, PerkinElmer, Japan) was used to evaluate the Luc-BMSC luminescence in mice at 1, 3, 5, and 7 days after the Luc-BMSC infusion ($n = 8$). The control group was infused 100 μl of PBS into the spleen ($n = 8$). The CDAA diet was continued after the infusion, and at 4 weeks after the Luc-BMSC infusion, the mice were sacrificed, and the liver and blood were collected (Fig. 2A).

Serum marker measurement. Blood was stored in a BD Microtainer SST (BD Bio-sciences, Franklin Lakes, NJ) and centrifuged ($1,200 \times g$ for 10 min) to separate the serum. The serum concentration of albumin (Alb), total bilirubin (T-bil), low-density lipoprotein (LDL), and high-density lipoprotein (HDL) was measured using a Hitachi 7180 automatic analyzer (Hitachi High-Tech Corporation, Tokyo, Japan). Alb was assayed using the Bromocresol Green method, T-bil was assayed using an enzymic method, and LDL and HDL were assayed using a direct method.

Immunohistochemistry. All immunostaining experiments used 3-μm paraffin-embedded sections of liver fixed with 4% paraformaldehyde (Wako). Immunostaining used the Vectastain ABC kit (PK-4001; Vector Laboratories, Burlingame, CA), and target proteins were detected using the avidin-biotin complex (ABC) method. The primary antibodies were anti-F4/80 (ab111101; Abcam, Tokyo, Japan), anti-inducible nitric oxide synthase (iNOS) (ab15323; Abcam), anti-CD163 (ab182422; Abcam), and anti-8-hydroxy-2'-deoxyguanosine (8-OHdG) (bs-1278R; Bioss Inc., Woburn, MA) antibodies. A fluorescence microscope (BIOREVO BZ-9000; Keyence, Osaka, Japan) captured the images of 5 sections from each mouse (5 mice from each group) at 100× magnification, and the number of positively stained cells was calculated using the BZ analyzer II (Keyence).

Histomorphometry. Histomorphometry was performed using an imaging system coupled to BIOREVO BZ-9000. The fibrotic area was calculated as the percent of Sirius red-stained area relative to the total sample using the BZ analyzer II (Keyence). Liver steatosis was evaluated by calculating the lipid droplet area in the liver and taking its proportion with respect to the total area. The vessels were excluded from this calculation. Using 8 mice from each group, we imaged 5 liver sections from each mouse at ×100 magnification and calculated the mean values.

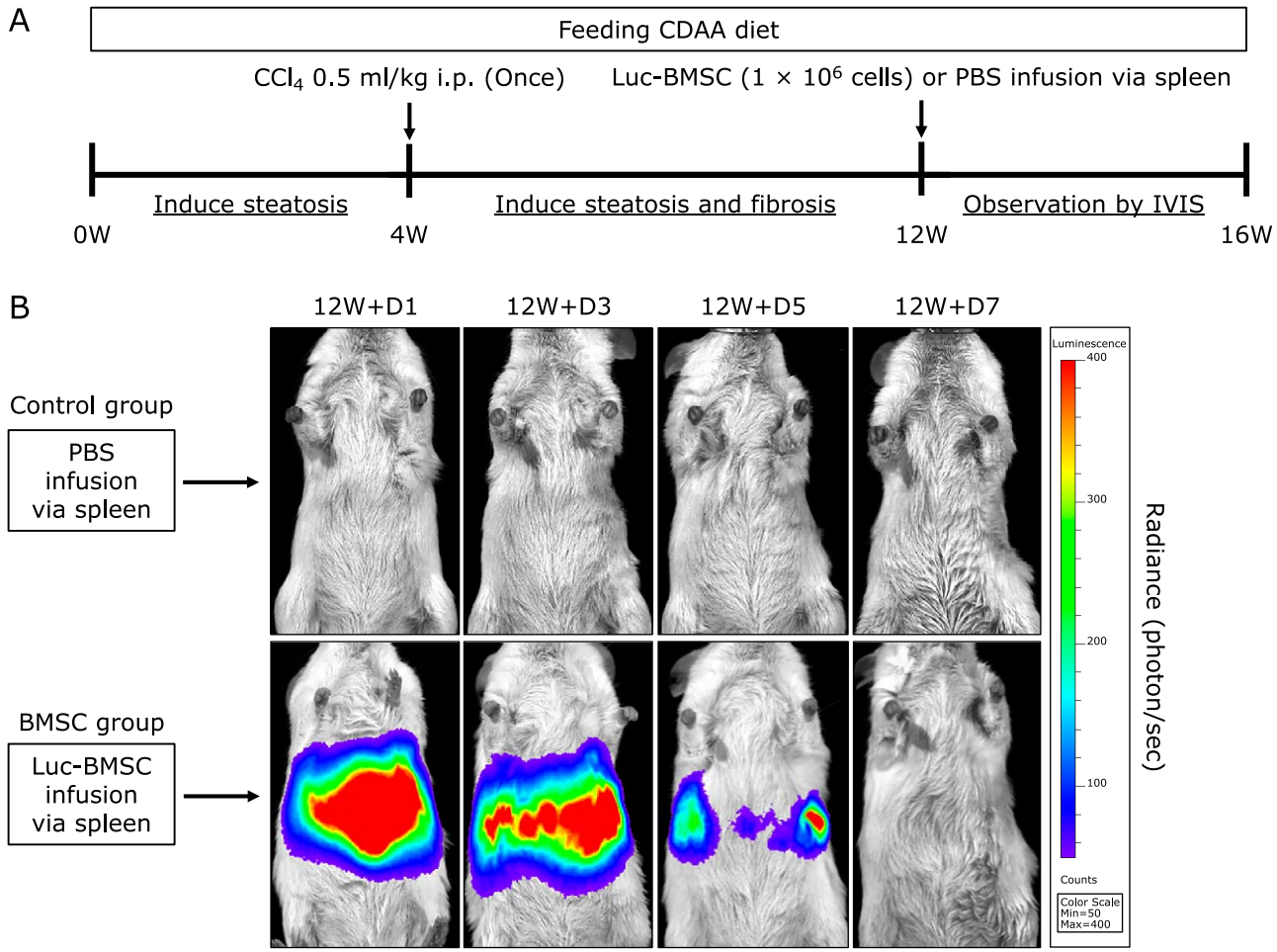

Fig. 2. Protocol for evaluating trans-portal hepatic infusion of cultured bone marrow-derived mesenchymal stem cells in a modified steatohepatitis murine model. (A) Experimental protocol. Mice are fed a choline-deficient L-amino acid-defined (CDAA) diet for 4 weeks and then injected a single intraperitoneal dose of carbon tetrachloride (CCl_4) at 0.5 ml/kg. The CDAA diet is continued thereafter, and, after 12 weeks of the CDAA diet (12W), syngeneic bone marrow-derived mesenchymal stem cells transduced to express luciferase [luciferase-positive bone marrow-derived mesenchymal stem cells (Luc-BMSC)] adjusted to 1.0×10^6 cells/100 μl are infused into the spleen. A control group is infused with phosphate-buffered saline (PBS) into the spleen. The *in vivo* dynamics of Luc-BMSC over time (at 1, 3, 5, and 7 days after Luc-BMSC infusion; 12W + D1, 12W + D3, 12W + D5, 12W + D7, respectively) are observed using the *in vivo* imaging system (IVIS), and, at 4 weeks after Luc-BMSC infusion (16W), the mice are sacrificed. (B) Evaluation of Luc-BMSC *in vivo* dynamics using the IVIS. PBS is infused into the spleen of a control group, 1.0×10^6 cells of Luc-BMSC in PBS are infused into the spleen of the BMSC group, and observations are taken over time from 1 day to 7 days after infusion (12W + D1 to 12W + D7). Images from a representative animal are shown.

Table 1. The primers used for real-time PCR

Genes	Forward (5'-3')	Reverse (5'-3')
Col1a1	CCCACCCAGCTCAGATTCA	GGCAATTAGAGTCAGCAGAAATACA
Cpt1a	GAAGCCTTTGGGTGGATATGTGA	ATGGAACTGGTGGCCAATGA
Ppara	ACTGTCCTTGGTGCCATCCTC	GGATGCTGGTATCGGCTCAATAA
Fas	ACATGGACAAAGAACCATTATGCT	CTGGTTTGCATTGCACTTGGTA
Acaca	TGATGGTACCACAGCCCATTACA	GGCAATCTCAGTTCAAGCCAGTC
Srebp1	AGCCTGGCCATCTGTGAGAA	CAGACTGGTACGGGCCACAA
Actb	CATCCGTAAAGACCTCTATGCCAAC	ATGGAGCCACCGATCCACA

Col1a1, Collagen1A1; *Cpt1a*, carnitine palmitoyltransferase 1A; *Ppara*, peroxisome proliferator-activated receptor-α; *Fas*, fatty acid synthase; *Acaca*, acetyl-CoA carboxylase α; *Srebp1*, sterol regulatory element binding protein-1; *Actb*, β-actin.

RT-PCR analysis. Total RNA extraction was performed on the right lobe of the liver using the RNeasy Mini kit (Qiagen GmbH, Hilden, Germany). For cDNA synthesis, ReverTra Ace qPCR RT Master Mix with gDNA Remover (Toyobo, Tokyo, Japan) was used as described in the manufacturer's manual. Variations in gene expression were analyzed using the Step One Plus real-time PCR system (Thermo Fisher Scientific) with SYBR green. Relative quantification of gene expression was performed using β-actin (*Actb*) as an internal control. The primers used in this study are listed in Table 1.

Western blot analysis. Western blotting was performed according to a standard method.[13] In brief, the cell lysis buffer

doi: 10.3164/jcbn.20-88

contained 62.5 mM Tris-HCl (pH 6.8), 4% SDS, and 200 mM dithiothreitol (#1610610; Bio-Rad Laboratories, Inc., Hercules, CA). Cell lysates were electrophoresed on 12% acrylamide gels (#456-1045; Bio-Rad Laboratories, Inc.). Anti-α-smooth muscle actin (α-SMA) antibody (ab5694; Abcam), anti-superoxide dismutase-2(SOD-2) antibody (ab13533; Abcam), anti-glyceraldehyde 3-phosphate dehydrogenase (GAPDH) antibody (ab9485; Abcam), or horseradish peroxidase-conjugated secondary antibodies (dilution 1:5,000, GE Healthcare, Chicago, IL) were used. Protein bands were detected by the ECL Plus Western Blotting Substrate (Thermo Fisher Scientific). The expression of the protein bands was normalized to that of GAPDH.

BMSC co-culture *in vitro*. The human hepatoblastoma cell line HepG2 cells were purchased from Summit Pharmaceuticals International (Tokyo, Japan). HepG2 cells were cultured in DMEM (Thermo Fisher Scientific) supplemented with 10% FBS (Thermo Fisher Scientific) and 100-μg/ml gentamicin (Thermo Fisher Scientific). HepG2 cells were seeded onto 12-well plates (Becton Dickinson Labware, NJ). To induce steatosis, HepG2 cells were exposed to 0.5-mM free fatty acid (FFA) mixture (oleic acid/palmitic acid, 2:1) (Sigma-Aldrich, St. Louis, MO) for 24 h. HepG2 cells were divided into the following two groups: 1) FFA-treated group; and 2) FFA and BMSC co-culture group. Then, 5×10^4 BMSCs were seeded onto the 0.4-μm-pore size Cell Culture Insert (Becton Dickinson Labware) and placed into the 12-well plate with the HepG2 cells that were initially seeded. In the transwell system, only secretome from BMSC cultured in the upper compartment could pass through the membrane to contact with HepG2 cells cultured in the lower compartment. After another 48 h, the cells were collected for Oil-red O staining (Sigma-Aldrich) and thereafter, incubated for 5 min in 100% isopropanol (Wako). The Oil-Red O staining solution was then extracted from each well, and absorbance at a wavelength of 492 nm was measured using the Infinite M 200Pro (Tecan, Kanagawa, Japan).

Statistical analysis. Data were analyzed using the Student's *t* test. *P* values of <0.05 were considered statistically significant. Data are presented as the mean ± SD.

Results

Development of the steatohepatitis murine model. Compared to the CDAA fed mice not injected with CCl_4 (control), injecting a single dose of CCl_4 to mice on the CDAA diet (BMSC) induced not only lipid deposition in the liver, but also inflammatory cell infiltration of liver lobules and fibrosis around the hepatocytes similar to the pericellular fibrosis (Fig. 1B).

BMSC migrated into the liver. A luciferin was injected from the caudal vein to induce fluorescence of Luc-BMSCs infused into the spleen, and the IVIS was used to observe the *in vivo* dynamics of Luc-BMSCs over time (Fig. 2A). The Luc-BMSCs infused into the spleen passed through the portal vein and reached the liver by 1 day after the infusion (12 weeks + 1 day: 12W + D1). There was no subsequent distribution of Luc-BMSCs throughout the body; instead, they remained accumulated in the liver and spleen, and *in vivo* fluorescence disappeared 7 days after cell infusion (12W + 7D). The time from cell infusion to disappearance of *in vivo* fluorescence was 3.9 ± 0.4 days ($n = 8$) (Fig. 2B).

BMSC infusion reduced liver fibrosis. Evaluation of liver fibrosis with Sirius red staining revealed a significantly lower positively-stained area in the BMSC group than in the control

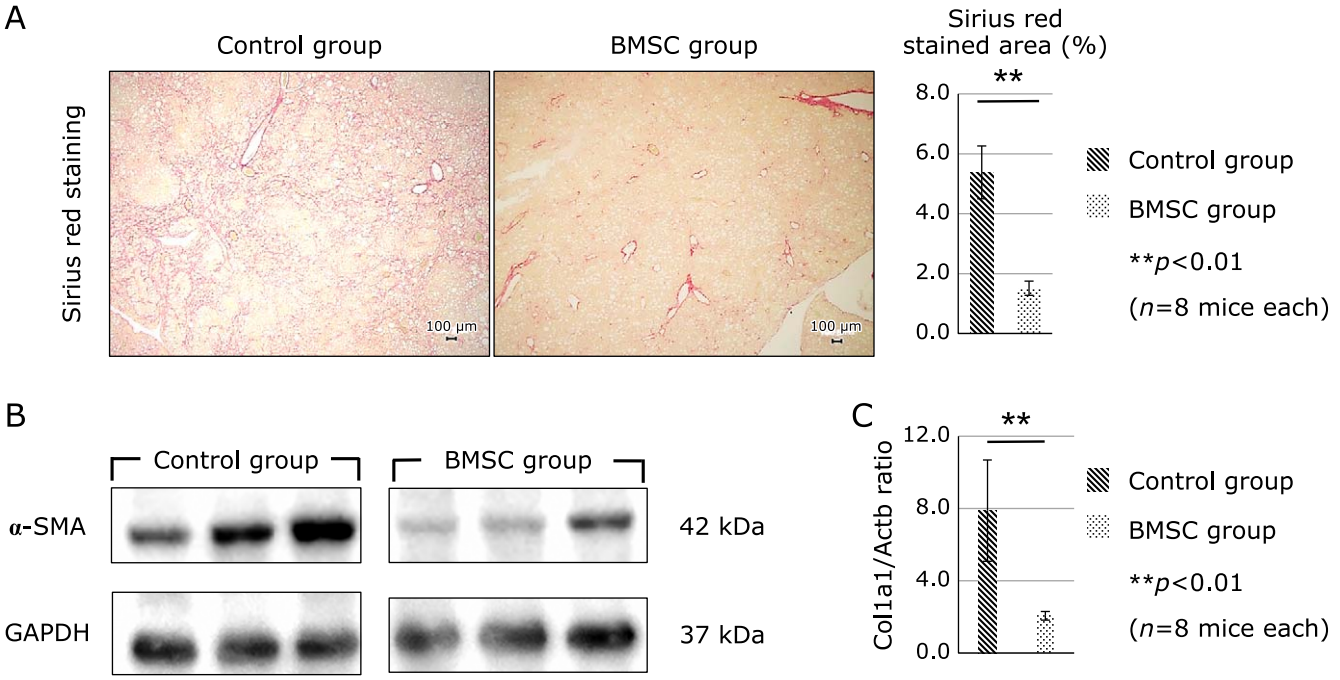

Fig. 3. Quantification of liver fibrosis. Luciferase positive bone marrow-derived mesenchymal stem cells (Luc-BMSCs) adjusted to 1.0×10^6 cells/100 μl were infused into the spleen of a modified steatohepatitis murine model at 12 weeks of the choline-deficient, L-amino acid-defined diet (12W), and at 4 weeks after infusion, the animals were sacrificed ($n = 8$). Liver fibrosis and liver steatosis were similarly induced in a control group that was infused with phosphate-buffered saline (PBS) into the spleen, and after 4 weeks, the animals were sacrificed ($n = 8$). The evaluation of liver fibrosis is shown. (A) The mean level of Sirius red-stained area was significantly lower in the BMSC group. Control group vs BMSC group = 5.4 ± 0.9% vs 1.5 ± 0.2%. Error bars indicate SD, $n = 8$ mice each. **p<0.01. Magnification ×40, scale bars = 100 μm. (B) Western blotting of α-smooth muscle actin (α-SMA) protein in the liver between the BMSC and control groups. Glyceraldehyde 3-phosphate dehydrogenase (GAPDH) protein was used as an internal control, $n = 3$ each. (C) mRNA expression of collagen1a1 (*Col1a1*) normalized with β-actin (*Actb*), $n = 8$ mice each. **p<0.01.

group (control group vs BMSC group = 5.4 ± 0.9% vs 1.5 ± 0.2%, n = 8 mice per group; p<0.01) (Fig. 3A). α-SMA protein in the liver (n = 3 mice per group) and the collagen 1A1 (*Col1a1)/Actb* ratio (n = 8 mice per group; p<0.01) were also both significantly suppressed in the BMSC group than in the control group (Fig. 3B and C).

BMSC infusion improved the serum biochemical markers. Blood biochemistry experiments revealed significant elevation of serum albumin (control group vs BMSC group = 2.3 ± 0.5 g/dl vs 3.0 ± 0.4 g/dl, n = 8 mice per group; p<0.01) and significant reduction of total serum bilirubin in the BMSC group compared to the control group (0.4 ± 0.3 mg/dl vs 0.1 ± 0.1 mg/dl, n = 8 mice per group; p<0.05). The LDL/HDL ratio also tended to be lower in the BMSC group (0.4 ± 0.4% vs 0.2 ± 0.1%, n = 8 mice per group; p = 0.11) (Table 2).

BMSC infusion reduced liver steatosis. The lipid droplet deposition area was significantly lower in the BMSC group (control group vs BMSC group = 34.7 ± 2.1% vs 21.2 ± 3.3%, n = 8 mice per group; p<0.01) (Fig. 4A). Peroxisome proliferator-activated receptor-α (*Ppara)* and carnitine palmitoyltransferase 1A (*Cpt1a*) expressions were also significantly increased in the BMSC group (n = 8 mice per group; p<0.01 and p<0.05, respectively), although there was no difference in the expression of fatty acid synthase (*Fas*), acetyl-CoA carboxylase α (*Acaca*), and sterol regulatory element binding protein-1 (*Srebp1*) between the groups (n = 8 mice per group) (Fig. 4B).

Table 2. Comparison of serum data 4 weeks after luciferase-positive bone marrow derived mesenchymal stem cells (Luc-BMSC) infusion

	Albumin (g/dl)	T-bil (mg/dl)	LDL/HDL
Control group	2.3 ± 0.5	0.4 ± 0.3	0.4 ± 0.4
BMSC group	3.0 ± 0.4**	0.1 ± 0.1*	0.2 ± 0.1

T-bil, total bilirubin; LDL, low density lipoprotein; HDL, high density lipoprotein. Data are means ± SD, n = 8 each. *p<0.05 vs control group, **p<0.01 vs control group.

BMSC infusion modulated macrophage polarization. There was no difference in the number of cells positive for the pan-macrophage marker F4/80 between the groups [control group vs BMSC group = 192.4 ± 19.4 vs 153.3 ± 19.9 cells/5 high power fields (HPFs) per mouse, n = 5 mice per group; not significant, Fig. 5A]. Meanwhile, significantly more cells were positive for the M1 macrophage marker iNOS in the control group (control group vs BMSC group = 84.9 ± 6.5 vs 12.4 ± 2.8 cells/5 HPFs per mouse, n = 5 mice per group; p<0.01, Fig. 5B), whereas significantly more cells were positive for the M2 macrophage marker CD163 in the BMSC group (control group vs BMSC

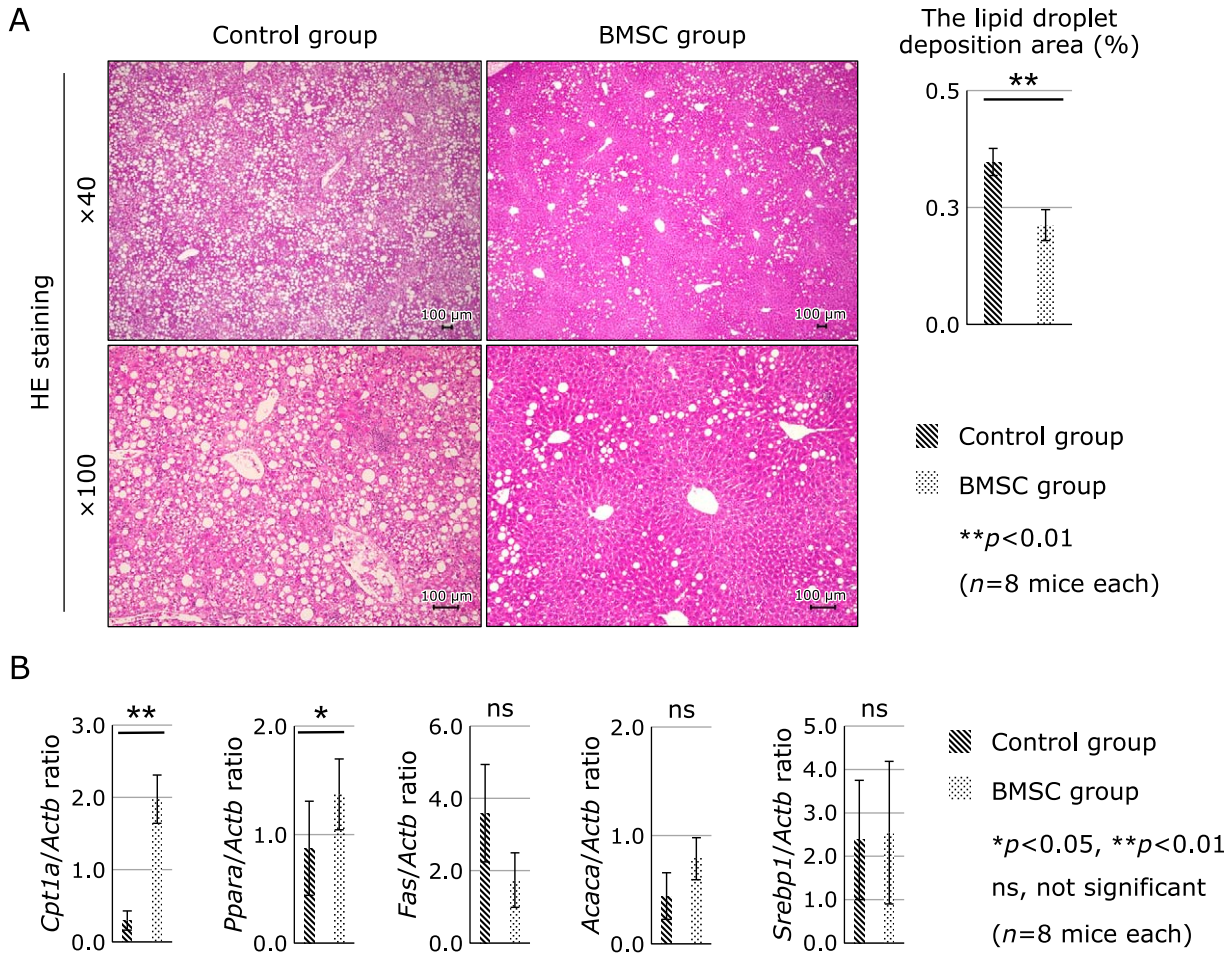

Fig. 4. Quantification of liver steatosis and lipid metabolism in the liver. Luciferase positive bone marrow-derived mesenchymal stem cells (Luc-BMSCs) adjusted to 1.0 × 10^6 cells/100 μl were infused into the spleen of a modified steatohepatitis murine model at 12 weeks of the choline-deficient, L-amino acid-defined diet (12W), and, at 4 weeks after infusion, the animals were sacrificed (n = 8). (A) Hematoxylin and eosin (HE) staining. The lipid droplet deposition area was significantly lower in the BMSC group (control group vs BMSC group = 34.7 ± 2.1% vs 21.2 ± 3.3%). Error bars indicate SD, n = 8 mice each. **p<0.01. Magnifications ×40 and ×100. (B) mRNA expressions of genes related to lipid metabolism in the liver. n = 8 mice each. *p<0.05, **p<0.01, ns, not significant. Error bars indicate SD.

doi: 10.3164/jcbn.20-88

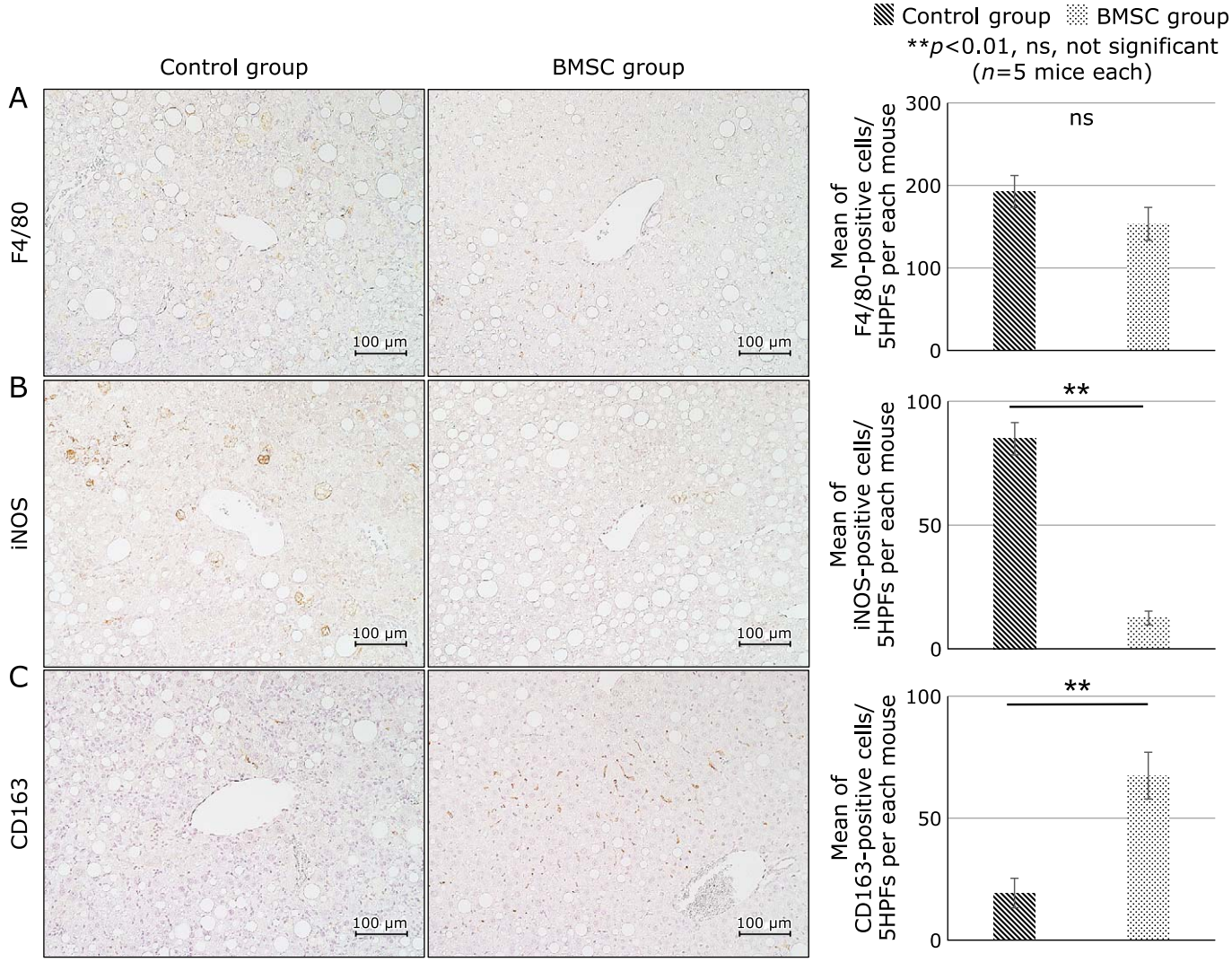

Fig. 5. Assessment of macrophage polarization. Representative images and quantification of (A) F4/80, (B) iNOS, and (C) CD163 immunostaining of the liver sections (magnification ×200). The mean number of immunostaining-positive cells is shown after staining and imaging 5 liver sections from each mouse (n = 5 mice per group) at 100× magnification. Scale bars = 100 μm. **p<0.01. ns, not significant. Error bars indicate SD.

group = 19.3 ± 6.0 vs 67.5 ± 9.6 cells/5 HPFs per mouse, n = 5 mice per group; p<0.01, Fig. 5C).

BMSC infusion maintained oxidative stress. Significantly fewer cells were 8-OHdG-positive in the BMSC group than in the control group (control group vs BMSC group = 68.6 ± 9.7 vs 36.4 ± 7.1 cells/5 HPFs per mouse, n = 5 mice per group; p<0.05, Fig. 6A). The expression of SOD-2 protein that acts against oxidative stress was also increased in the BMSC group (n = 3 mice per group) (Fig. 6B).

HepG2 co-culture with BMSCs showed reduced steatosis *in vitro*. HepG2 cells with induced lipid accumulation were co-cultured with BMSCs, and after 48 h, lipid deposition in the HepG2 cells was evaluated by Oil-red O staining (Fig. 7A). Hence, HepG2 cells co-cultured with BMSCs contained significantly lesser lipid deposition than the control group, and measuring the absorbance of the Oil-red O staining solution extracted from each well at 492 nm revealed significantly lower absorbance in the group co-cultured with BMSCs (control group vs BMSC co-culture group = 1.4 ± 0.1 vs 1.2 ± 0.1, n = 12 per group; p<0.01, Fig. 7B).

Discussion

We previously reported the safety and efficacy of the infusion of cultured autologous BMSCs into a peripheral vein or the hepatic artery of CCl_4-induced liver fibrosis animal models.[1–6] Here, we confirmed that trans-portal hepatic infusion of BMSCs improved the liver fibrosis, liver steatosis, and oxidative stress in the steatohepatitis murine model.

Given that liver fibrosis is reportedly the most important factor for liver disease-related deaths in cases of NAFLD and NASH,[9–11] suppressing liver fibrosis is an important topic. Although there have been several reports of BMSCs improving liver steatosis and liver fibrosis in mouse and rat models of NASH,[14–16] there remain many uncertainties concerning the *in vivo* dynamics of infused BMSCs and the mechanism of their therapeutic effects on liver steatosis and liver fibrosis. Here, BMSCs infused from the spleen migrated through the portal vein into the liver, where they remained without being distributed throughout the body and disappeared from the body at 3.9 ± 0.4 days after infusion. Banas *et al.*[17] have reported liver function improvement after infused BMSCs differentiated into hepatocytes. However, the

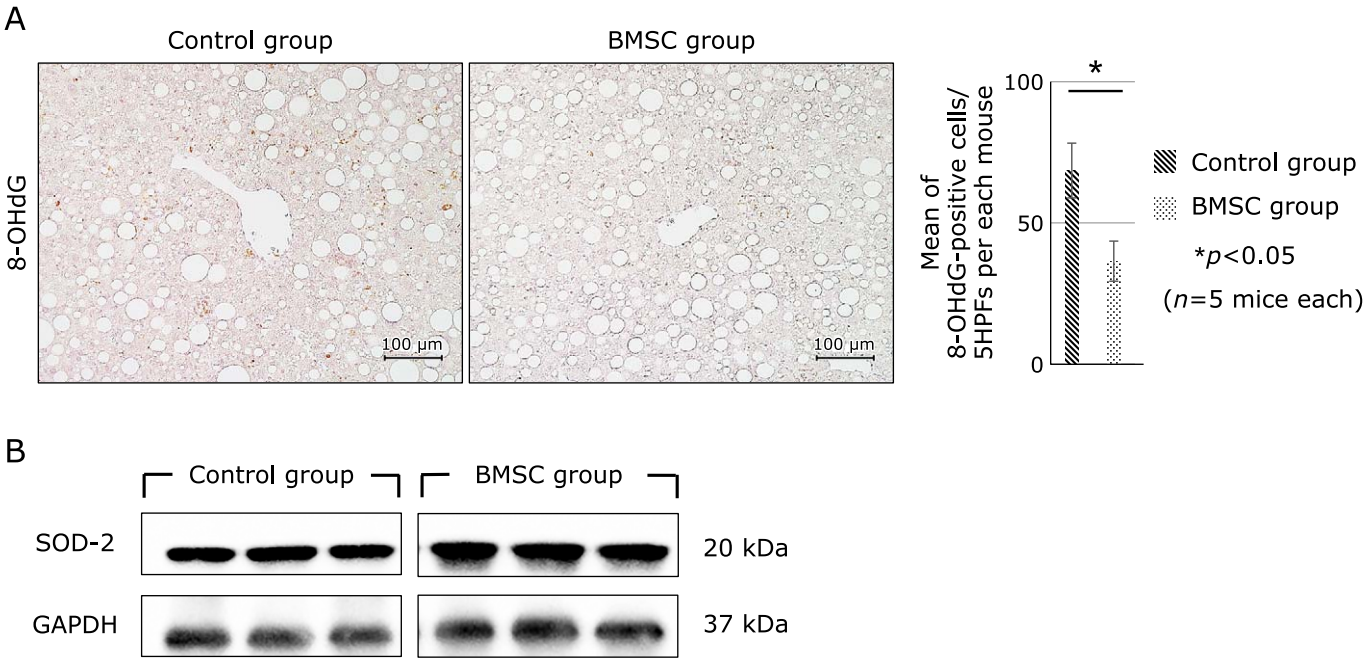

Fig. 6. Assessment of oxidative stress. (A) Representative images and quantification of 8-hydroxy-2'-deoxyguanosine (8-OHdG) immunostaining of the liver sections (magnification ×200). The mean number of immunostaining-positive cells is shown after staining and imaging 5 liver sections from each mouse (n = 5 mice per group) at 100× magnification. Scale bars = 100 μm. *p<0.05. Error bars indicate SD. (B) Western blotting of superoxide dismutase-2 (SOD-2) in the liver between the control and BMSC groups. Glyceraldehyde 3-phosphate dehydrogenase (GAPDH) protein was used as an internal control, n = 3 each.

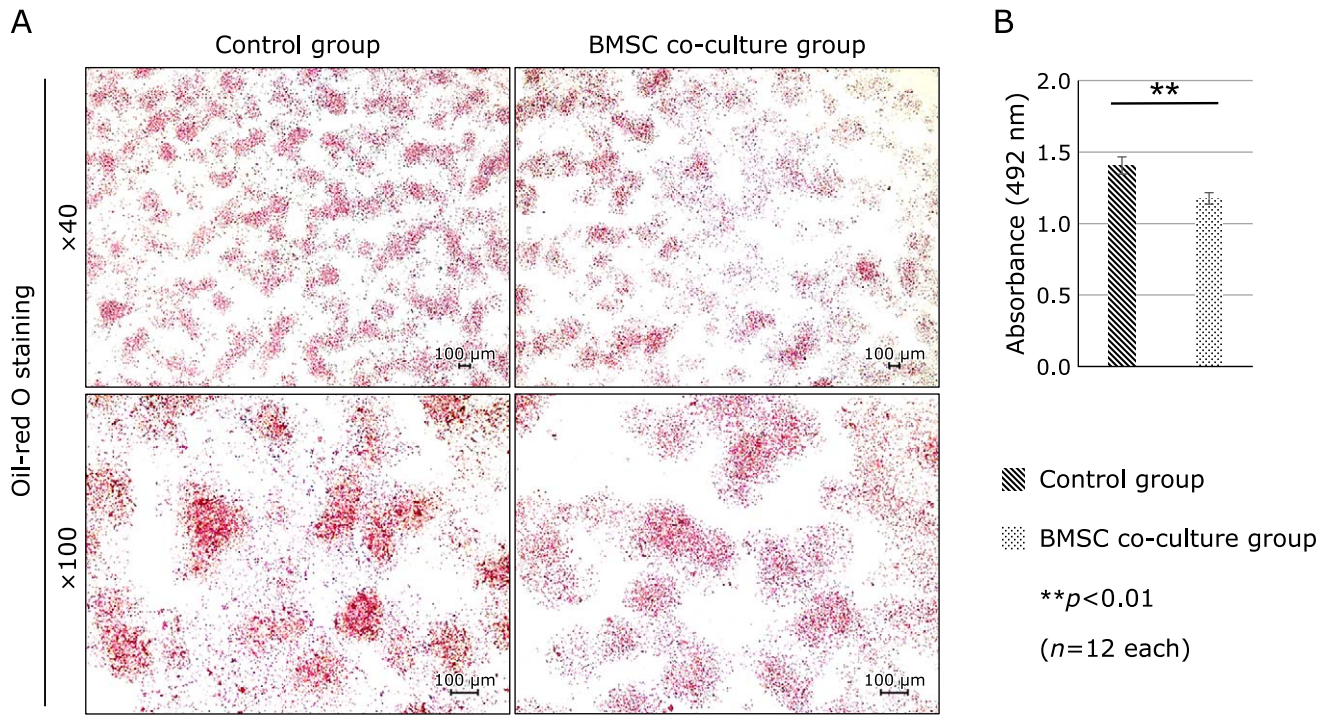

Fig. 7. Assessment of the effects of cultured bone marrow-derived mesenchymal stem cells (BMSCs) on steatosis in HepG2 cells. (A) Oil-red O staining of HepG2 cells (magnification ×40, ×100). Control group: HepG2 cells were exposed to 0.5 mM free fatty acid (FFA) mixture for 72 h in the 12-well plate. BMSC co-culture group: HepG2 cells were exposed to 0.5 mM FFA mixture for 24 h. Then, 5×10^4 BMSCs were seeded onto the 0.4-μm-pore size Cell Culture Insert and placed into the 12-well plate with the HepG2 cells, and these two kinds of cells were cultured for another 48 h. Scale bars = 100 μm. (B) Absorbance (492 nm) of Oil-red O staining solution. The mean absorbance at 492 nm of Oil-red O staining solution extracted from wells is shown (n = 12 per group). Control group vs BMSC co-culture group = 1.4 ± 0.1 vs 1.2 ± 0.1. Error bars indicate SD, n = 12 each, **p<0.01.

doi: 10.3164/jcbn.20-88

present study suggests a different mechanism of BMSC action, with BMSCs acting on other cells normally present in the liver (macrophages and hepatocytes) and improving fibrosis and steatosis through cell-cell interaction.

Macrophages play a role in NASH onset, and there are reports showing that MSCs with anti-inflammatory effects improved fibrosis and steatosis by acting on macrophages.[18–21] Our study showed that M1 macrophages in the liver switched phenotype to M2 macrophages, and there was a substantial change in macrophage distribution. Reports have shown that a reduction in M1 macrophages and an increase in M2 macrophages improved liver fibrosis both *in vivo* and *in vitro* by suppressing the inflammatory cytokines, interleukin (IL)-6 and IL-1β, releasing the antifibrotic factor IL-10, inhibiting the activity of hepatic stellate cells, and increasing the levels of the extracellular matrix degrading enzymes, such as matrix metalloproteinase (MMP)-9 and MMP-12.[22–25] Griess *et al.*[26] have also reported that M2 macrophages increased the levels of SOD-2, a protein effective against oxidative stress, suggesting that, in the present study, increased M2 macrophages caused an increase in SOD-2 protein, which controlled intrahepatic oxidative stress, thereby reducing the number of 8-OHdG-positive cells in the liver.

The present study also confirmed that BMSC infusion improved liver steatosis. In a CDAA diet model, the synthesized amount of phosphatidylcholine, which uses choline as a substrate, decreases, thereby suppressing the secretion of hydrophobic triglyceride-rich very-low-density lipoprotein from hepatocytes and inducing lipid deposition in the liver.[27] Here, we did not observe any changes in gene expression indicative of lipid synthesis (FAS, ACACA, and SREBP1) in the BMSC group; instead, we noted an increase in gene expression indicative of lipid metabolism (PPARα and CPT-1). Lee *et al.*[15] have reported that transplantation of adipocyte-derived human MSCs increased the PPARα and PPARγ expressions in obese mice, and the CPT-1 gene is a known target of PPARα.[28] In our study, this suggests that BMSC infusion increased the CPT-1 expression via PPARα, which increased the beta-oxidation in the mitochondria and improved liver steatosis. The improvement in the lipid accumulation in the HepG2 cells owing to the co-culture with BMSCs *in vitro* also confirms that BMSCs have an ameliorating effect on liver steatosis.

Although our results provided evidence of the therapeutic effects of BMSC, several limitations should be mentioned. We found decreased M1 macrophages and increased M2 macrophages in the BMSC group, although we did not confirm direct evidence on the macrophage phenotypic switch. The treatment with BMSC may increase recruitment of M2 macrophages in the liver; however, it remains unclear whether and how the increased the proportion of M2 macrophages actually contributed to liver fibrosis, liver steatosis, and oxidative stress. Further studies are, therefore, necessary to explore how the BMSCs regulate M1/M2 polarization and improve liver fibrosis and liver steatosis.

In conclusion, we confirmed the efficacy of trans-portal hepatic infusion of BMSCs in a steatohepatitis murine model.

Author Contributions

Conceived and designed the experiments: RS, TT, and IS. Performed the experiments: RS and TT. Analyzed the data: RS and TT. Contributed reagents/materials/analysis tools: RS, KF, TM, TI, NY, and TT. Wrote the paper: RS, TM, and TT.

Acknowledgments

We would like to thank Ms. Mariko Yamada, Ms. Risa Mochizuki, and Ms. Kumie Ota for their technical assistance. This study was supported by The Project Promoting the Research and Development (R&D) Center on Regenerative Medicine in Yamaguchi Prefecture and by JSPS KAKENHI grants to IS (grant number: JP17H04162) and TT (grant number: JP17K09428).

Abbreviations

ABC	avidin-biotin complex
ACACA	acetyl-CoA carboxylase α
Alb	albumin
α-SMA	α-smooth muscle actin
BMSCs	autologous bone marrow-derived mesenchymal stem cells
CCl_4	carbon tetrachloride
CDAA	choline-deficient, L-amino acid defined
CPT-1	carnitine palmitoyltransferase 1
DAA	direct-acting antiviral
DMEM	Dulbecco's Modified Eagle medium
FAS	fatty acid synthase
FBS	fetal bovine serum
FFA	free fatty acid
GAPDH	glyceraldehyde 3-phosphate dehydrogenase
HBV	hepatitis B virus
HCV	hepatitis C virus
HDL	high-density lipoprotein
HPFs	high power fields
IL	interleukin
iNOS	inducible nitric oxide synthase
LDL	low-density lipoprotein
Luc-BMSC	luciferase-positive syngeneic BMSCs
MMP	matrix metalloproteinase
NAFLD	nonalcoholic fatty liver disease
NAs	nucleoside/nucleotide analogs
NASH	nonalcoholic steatohepatitis
8-OHdG	8-hydroxy-2'-deoxyguanosine
PBS	phosphate-buffed saline
PPAR	peroxisome proliferator-activator receptor
SOD-2	superoxide dismutase-2
SREBP1	sterol regulatory element binding protein-1
T-bil	total bilirubin

Conflict of Interest

No potential conflicts of interest were disclosed.

References

1 Sakaida I, Terai S, Yamamoto N, *et al*. Transplantation of bone marrow cells reduces CCl_4-induced liver fibrosis in mice. *Hepatology* 2004; **40**: 1304–1311.
2 Terai S, Ishikawa T, Omori K, *et al*. Improved liver function in patients with liver cirrhosis after autologous bone marrow cell infusion therapy. *Stem Cells* 2006; **24**: 2292–2298.
3 Iwamoto T, Terai S, Mizunaga Y, *et al*. Splenectomy enhances the anti-fibrotic effect of bone marrow cell infusion and improves liver function in cirrhotic mice and patients. *J Gastroenterol* 2012; **47**: 300–312.
4 Tanimoto H, Terai S, Taro T, *et al*. Improvement of liver fibrosis by infusion of cultured cells derived from human bone marrow. *Cell Tissue Res* 2013; **354**: 717–728.
5 Matsuda T, Takami T, Sasaki R, *et al*. A canine liver fibrosis model to develop a therapy for liver cirrhosis using cultured bone marrow-derived cells. *Hepatol Commun* 2017; **1**: 691–703.
6 Nishimura T, Takami T, Sasaki R, *et al*. Liver regeneration therapy through the hepatic artery-infusion of cultured bone marrow cells in a canine liver fibrosis model. *PLoS One* 2019; **14**: e0210588.
7 Lade A, Noon LA, Friedman SL. Contributions of metabolic dysregulation and inflammation to nonalcoholic steatohepatitis, hepatic fibrosis, and cancer.

Curr Opin Oncol 2014; **26**: 100–107.
8 Bellentani S. The epidemiology of non-alcoholic fatty liver disease. *Liver Int* 2017; **37 Suppl 1**: 81–84.
9 Ekstedt M, Hagström H, Nasr P, *et al*. Fibrosis stage is the strongest predictor for disease-specific mortality in NAFLD after up to 33 years of follow-up. *Hepatology* 2015; **61**: 1547–1554.
10 Angulo P, Kleiner DE, Dam-Larsen S, *et al*. Liver fibrosis, but no other histologic features, is associated with long-term outcomes of patients with nonalcoholic fatty liver disease. *Gastroenterology* 2015; **149**: 389–397.
11 Dulai PS, Singh S, Patel J, *et al*. Increased risk of mortality by fibrosis stage in nonalcoholic fatty liver disease: systematic review and meta-analysis. *Hepatology* 2017; **65**: 1557–1565.
12 Komiya C, Tanaka M, Tsuchiya K, *et al*. Antifibrotic effect of pirfenidone in a mouse model of human nonalcoholic steatohepatitis. *Sci Rep* 2017; **7**: 44754.
13 Fujisawa K, Hara K, Takami T, *et al*. Evaluation of the effects of ascorbic acid on metabolism of human mesenchymal stem cells. *Stem Cell Res Ther* 2018; **9**: 93.
14 Winkler S, Borkham-Kamphorst E, Stock P, *et al*. Human mesenchymal stem cells towards non-alcoholic steatohepatitis in an immunodeficient mouse model. *Exp Cell Res* 2014; **326**: 230–239.
15 Lee CW, Hsiao WT, Lee OKS. Mesenchymal stromal cell-based therapies reduce obesity and metabolic syndromes induced by a high-fat diet. *Transl Res* 2017; **182**: 61–74.e8.
16 Cao M, Pan Q, Dong H, *et al*. Adipose-derived mesenchymal stem cells improve glucose homeostasis in high-fat diet-induced obese mice. *Stem Cel Res Ther* 2015; **6**: 208.
17 Banas A, Teratani T, Yamamoto Y, *et al*. Adipose tissue-derived mesenchymal stem cells as a source of human hepatocytes. *Hepatology* 2007; **46**: 219–228.
18 Itoh M, Suganami T, Kato H, *et al*. CD11c$^+$ resident macrophages drive hepatocyte death-triggered liver fibrosis in a murine model of nonalcoholic steatohepatitis. *JCI Insight* 2017; **2**: e92902.
19 Nakashima H, Nakashima M, Kinoshita M, *et al*. Activation and increase of radio-sensitive CD11b$^+$ recruited Kupffer cells/macrophages in diet-induced steatohepatitis in FGF5 deficient mice. *Sci Rep* 2016; **6**: 34466.
20 Krenkel O, Puengel T, Govaere O, *et al*. Therapeutic inhibition of inflammatory monocyte recruitment reduces steatohepatitis and liver fibrosis. *Hepatology* 2018; **67**: 1270–1283.
21 Wan J, Benkdane M, Teixeira-Clerc F, *et al*. M2 Kupffer cells promote M1 Kupffer cell apoptosis: a protective mechanism against alcoholic and nonalcoholic fatty liver disease. *Hepatology* 2014; **59**: 130–142.
22 Baeck C, Wehr A, Karlmark KR, *et al*. Pharmacological inhibition of the chemokine CCL2(MCP-1) diminishes liver macrophage infiltration and steatohepatitis in chronic hepatic injury. *Gut* 2012; **61**: 416–426.
23 Zhou YZ, Cheng Z, Wu Y, *et al*. Mesenchymal stem cell-derived conditioned medium attenuate angiotensin Ⅱ-induced aortic aneurysm growth by modulating macrophage polarization. *J Cell Mol Med* 2019; **23**: 8233–8245.
24 Cho DI, Kim MR, Jeong HY, *et al*. Mesenchymal stem cells reciprocally regulate the M1/M2 balance in mouse bone marrow-derived macrophages. *Exp Mol Med* 2014; **46**: e70.
25 Calvente CJ, Tameda M, Johnson CD, *et al*. Neutrophils contribute to spontaneous resolution of liver inflammation and fibrosis via microRNA-223. *J Clin Invest* 2019; **130**: 4091–4109.
26 Griess B, Mir S, Datta K, Teoh-Fitzgerald M. Scavenging reactive oxygen species selectively inhibits M2 macrophage polarization and their pro-tumorigenic function in part, via Stat 3 suppression. *Free Radic Biol Med* 2020; **147**: 48–60.
27 Sha W, da Costa KA, Fischer LM, *et al*. Metabolomic profiling can predict which humans will develop liver dysfunction when deprived of dietary choline. *FASEB J* 2010; **24**: 2962–2975.
28 Mascaró C, Acosta E, Ortiz JA, Marrero PF, Hegardt FG, Haro D. Control of human muscle-type carnitine palmitoyltransferase I gene transcription by peroxisome proliferator-activated receptor. *J Biol Chem* 1998; **273**: 8560–8563.

doi: 10.3164/jcbn.20-88